APPLIED ORGANOMETALLIC CHEMISTRY
Appl. Organometal. Chem. **14**, 14–24 (2000)

New Molecular Compound Precursor for Aluminum Chemical Vapor Deposition

Tsutomu Shinzawa[1]*, Fumihiko Uesugi[2], Iwao Nishiyama[3], Kazumi Sugai[1], Shunji Kishida[4] and Hidekazu Okabayashi[5]
[1]ULSI Device Development Laboratory, NEC Corporation, 1120 Shimokuzawa, Sagamihara, Kanagawa 229-1134, Japan
[2]Device Analysis Technology Laboratories, NEC Corporation, 1753 Shimonumabe, Nakahara, Kawasaki, Kanagawa 211-0011, Japan
[3]Silicon Systems Research Laboratories, NEC Corporation, 34 Miyukigaoka, Tsukuba, Ibaraki 305-8501, Japan
[4]Resources and Environment Protection Research Laboratories, NEC Corporation, 4-1-1 Miyazaki, Miyamae-ku, Kawasaki 216-0033, Japan
[5]Research and Development Group, NEC Corporation, 34 Miyukigaoka, Tsukuba, Ibaraki 305-8501, Japan

A new type of precursor for aluminum chemical vapor deposition (Al-CVD) has been developed by mixing dimethylaluminum hydride (DMAH) and trimethylaluminum (TMA). The new precursor has proven itself to be effective for Al-CVD, where a good selectivity between the Si and the SiO_2 mask, a 3.0 $\mu\Omega$ cm resistivity and a pure Al film with low C and O contamination levels (under 100 ppm) were achieved. Quadrupole mass and infrared absorption analysis have shown that the precursor contains a new molecular compound, consisting of a DMAH monomer and a TMA monomer. The mixture has lower viscosity than DMAH and can be easily bubbled for a stable precursor vapor supply. Copyright © 2000 John Wiley & Sons, Ltd.

Keywords: chemical vapor deposition; aluminum; trimethylaluminum; dimethylaluminum hydride; precursor; quadrupole mass spectroscopy (QMS); FTIR; *ab initio* calculations

Received 2 February 1999; accepted 31 May 1999

* Correspondence to: Tsutomu Shinzawa, ULSI Device Development Laboratory, NEC Corporation, 1120 Shimokuzawa, Sagamihara, Kanagawa 229-1134, Japan.

INTRODUCTION

The filling of high-aspect-ratio contact holes with metal is indispensable in multilevel metallization for an ultra-large-scale integrated circuit (ULSI). For this purpose, aluminum selective and blanket CVDs are foreseen as hopeful candidates for contact hole filling. In the initial stage of CVD research, trimethylaluminum (TMA) was used as a CVD precursor. However, only aluminum carbide film was formed through the pyrolysis of this CVD gas.[1] The first success in metallic aluminum growth and blanket Al-CVD was reported using triisobutylaluminum (TIBA) as a CVD precursor.[2,3] However, when TIBA is used the surface morphology is not suitable for ULSI application because its nucleation density is low. Selective Al-CVD was first reported using TIBA.[4] Morphology problems have been partly overcome by using the double-wall CVD system,[5] but a low deposition rate due to the low vapor pressure of TIBA is still a problem. Reports have been published on aluminum-selective CVD with relatively high deposition rates and highly conductive film using dimethylaluminum hydride (DMAH).[6,7]

The disadvantage of DMAH as a CVD precursor is its high viscosity, which causes difficulty in bubbling DMAH in a conventional vessel. In order to decrease the DMAH viscosity and to increase the flow rate of the precursor, we tried to mix it with a solvent having lower viscosity and high vapor pressure. The liquid mixture of DMAH and TMA showed low viscosity and high vapor pressure. In addition the vapor from the mixture showed almost the same properties, such as selectivity, sheet

 CCC 0268–2605/2000/010014–11 $17.50

resistance, and film contamination level, as a pure DMAH vapor. Therefore, the liquid mixture was found to have great advantages (low viscosity and good film quality) as a CVD precursor. However, the reason why the liquid mixture shows almost the same properties as DMAH is not clear.

The vapor pressure of TMA is ten times higher than that of DMAH at room temperature. If the gas-phase precursor of the mixture consists of DMAH and TMA gas in proportions corresponding to their partial vapor pressure, TMA gas will be the dominant ingredient of the precursor vapor. This should result in poorly conductive Al film but actually we found that the film had almost the same conductivity as that obtained by using pure DMAH. We think that this was caused by a new molecular product being formed in the mixture gas. Therefore we investigated this new molecular product.

This paper provides a detailed characterization of the new molecular compound. The TMA and DMAH vapor mixture was investigated, using quadrupole mass spectroscopy (QMS) and FTIR (Fourier transform infrared spectroscopy) analysis. The quadrupole mass analysis revealed the fragment patterns of the new compound in the vapor mixture and was used to determine its molecular weight, which, in turn, suggested its structure. The molar fraction of the new compound in the mixture vapor was estimated, based on the FTIR analysis. The total energy and vibrational frequency of the new compound suggested by mass analysis were evaluated by *ab-initio* molecular orbital calculations.

EXPERIMENTAL

DMAH and TMA were prepared by Tosoh–Akzo Industries Ltd and used with no further purification in this work. Vapor pressures were 1.9 Torr for DMAH and 11.6 Torr for TMA at 298 K.[8,9] For QMS and FTIR analysis and CVD, the mixture of TMA and DMAH was prepared by mixing liquid TMA and liquid DMAH in a nitrogen gas atmosphere at room temperature, and was not submitted to purification.

The CVD apparatus consisted of a growth chamber with a mechanical booster pump system and a load-locked preparation chamber with a turbo-molecular pump system.[6] When the growth chamber was pumped out by the mechanical booster pump system, its base pressure was 1.33×10^{-2} Pa. The substrate, placed on a carbon susceptor, was heated to 450 °C. The substrates were 4-inch (10-cm) Si wafers. A subset of these wafers had SiO_2 patterns on the surface. The wafers were treated just before deposition by dipping briefly in dilute HF solution (H_2O / HF = 60:1) to remove native oxide on Si, rinsing with de-ionized water and blowing dry with a N_2. After a wafer had been placed in the load-locked chamber, the chamber was pumped to 1.33×10^{-5} Pa, and the wafer was transferred to the growth chamber. To reduce the water on the wafer it was baked at 300 °C in purified H_2 gas. The vapor mixture carried by hydrogen was then introduced into the growth chamber to deposit aluminum.

In order to identify the new compound in the DMAH and TMA mixture in the gas phase, mass spectra were measured using a molecular-beam type of ultra-high vacuum apparatus.[10,11] The liquid DMAH, TMA or a DMAH/TMA mixture was bubbled with a He carrier gas (research grade) and then the vapor was injected through a nozzle into a vacuum chamber. To avoid the formation of clusters by adiabatic expansion, a large-diameter (1 mm i.d.) nozzle was used. The effusive molecular beam was collimated with three orifices which were pumped separately, and then introduced into the QMS chamber. The QMS ionization energy was 70 eV. The background and operating pressures of the mass chamber were 10^{-10} and 10^{-8} Torr.

In order to confirm the new compound structure and evaluate its concentration in the vapor from the TMA and DMAH mixture, FTIR spectra were measured for the vapor from TMA, DMAH and the DMAH/TMA (70:30 mol/mol) mixture. In these measurements, about 0.2 ml aluminum alkyl compounds were injected into a cell 10 cm long with KBr windows in a nitrogen atmosphere. Each vapor had a saturated vapor pressure at room temperature. The infrared absorption spectra for these compounds were measured by an FTIR spectrometer, in the wavenumber range between 400 and 4000 cm^{-1} at room temperature.

MOLECULAR ORBITAL CALCULATIONS

The equilibrium geometry of each molecule was fully optimized as the Hartree–Fock level using the analytical gradient method.[12] The electron correlation energy was estimated by the second-order Moller–Plesset perturbation theory.[13,14] The basis

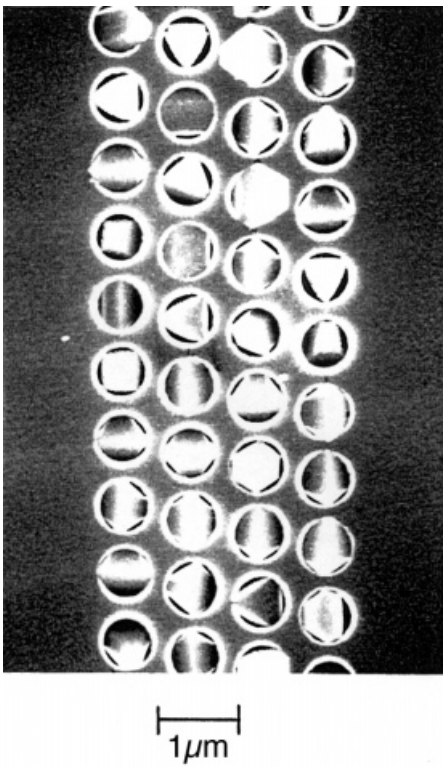

Figure 1 SEM micrograph of CVD aluminum for contact holes using a DMAH/TMA mixture as precursor gas. Al was selectively deposited on the contact-bottom silicon surface, while no film was grown on SiO_2 mask.

sets used in the present study were the 6–31*G*** split-valence polarization sets, which include one set of six *d*-polarization functions on non-hydrogen atoms and an additional set of *p*-polarization functions on hydrogen atoms.[15] The vibrational frequency analysis was performed to obtain zero-point vibrational energies and to assign the IR vibrational spectrum as discussed below under 'FTIR calculation'. The program for *ab-initio* molecular orbital calculations was Gaussian 94.[16]

RESULTS AND DISCUSSION

CVD characteristics using new precursor

The TMA/DMAH mixture (3:7 in liquid mixture) was examined in terms of its CVD characteristics concerning selectivity and Al-film quality. Individual CVD experiments were carried out under the following conditions: total pressure 270 Pa, precursor vessel temperature 30 °C, substrate temperature 240 °C, and deposition time 100 s. Using the vapor from the mixture as the CVD precursor gas, Al-CVD revealed good selectivity between the Si and the SiO_2 mask, as shown in Fig. 1. The aluminum grains show a facet-like shape grown over the contact holes, which implies single-crystal growth on the Si. Each facet plane does not always have the same orientation, which suggests that Al grain growth was not epitaxial on Si. Al deposition rates from both the TMA/DMAH mixture and the pure DMAH showed the same order.

To obtain the electrical resistivity, the sheet resistance was measured with a four-point probe and the film thickness was measured by the stylus method. The aluminum film deposited on Si using the new precursor shows a rather low resistivity of 3.0 $\mu\Omega$ cm (bulk Al resistivity is 2.7 $\mu\Omega$ cm at room temperature).

Impurities included in the grown Al film were measured by secondary ion mass spectroscopy (SIMS). The SIMS depth profile of the Al film is shown in Fig. 2. Atomic concentrations are shown for hydrogen, carbon and oxygen on the left-hand ordinate, and secondary ion counts are shown for Si and Al on the right-hand ordinate. Depth was evaluated by Ar sputter time, and dimple depth was measured by the stylus method. Significant amounts of H, C and O atoms are observed in Al the film from the surface to a depth of 0.2 μm. From 0.2 to 0.35 μm, both C and O contamination levels were lower than 100 ppm when surface contamination, caused by exposure to the atmosphere, was avoided. This level of contamination in Al film is the same as in films using DMAH. These results show that this new precursor has the same potential as good CVD precursor as DMAH.

Characterization of new precursor

QMS measurement and fragmentation pattern analysis

Figure 3 shows mass spectra for (a) TMA, (b) DMAH and (c) a DMAH/TMA mixture (1:1). Mass peaks at $m/z = 17$ (OH^+), 18 (H_2O^+), 19 (F^+), 28 (N_2^+ or CO^+) and 44 (CO_2^+) come from background impurities, because these peaks appeared when the vapor had flowed away. Other peaks that appeared in the mass number range between 12 and 57 for these vapors are not included in the analysis in the following discussion because these vapors have common fragment mass numbers.

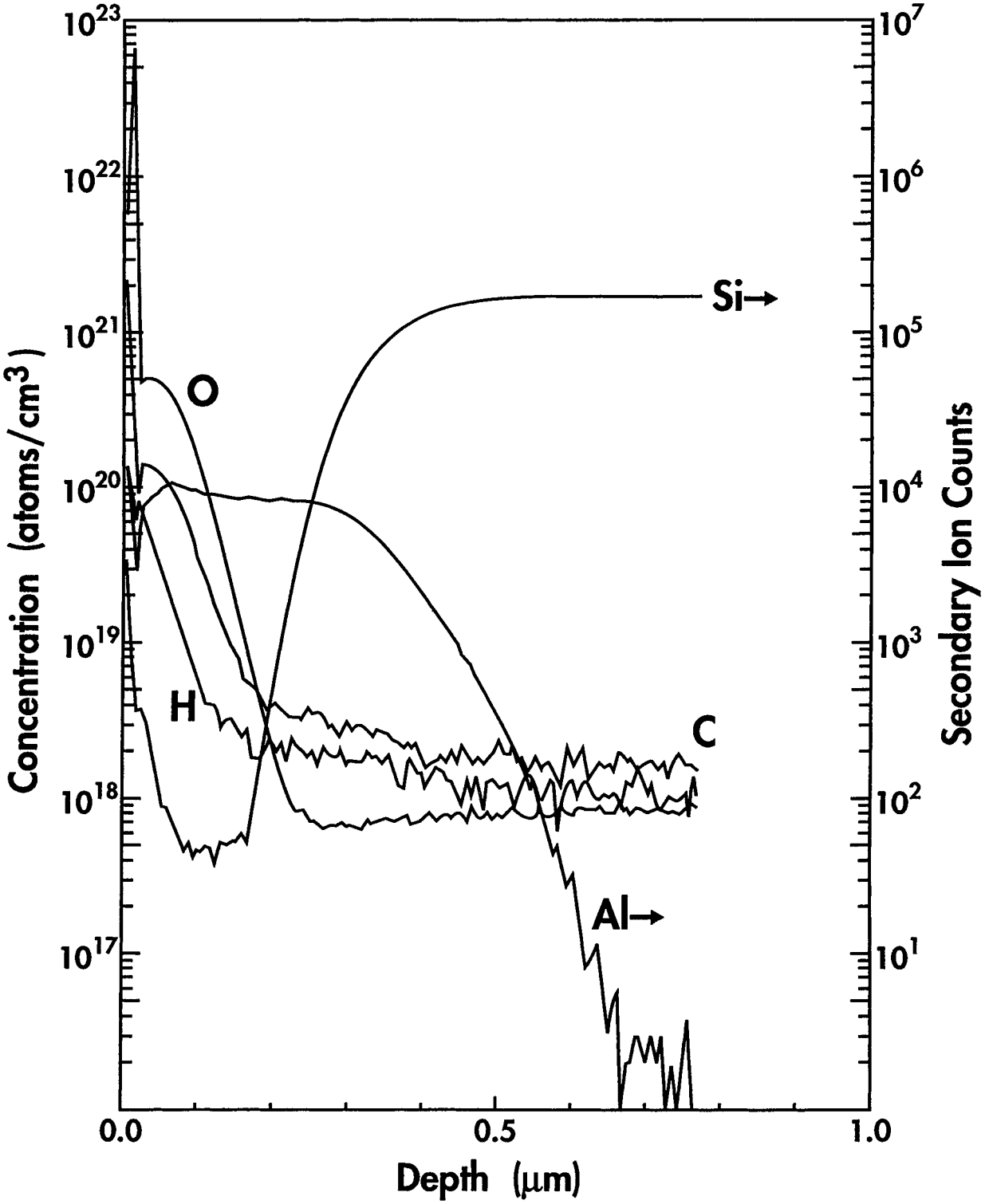

Figure 2 SIMS depth profile for Al film deposited using the DMAH/TMA mixture.

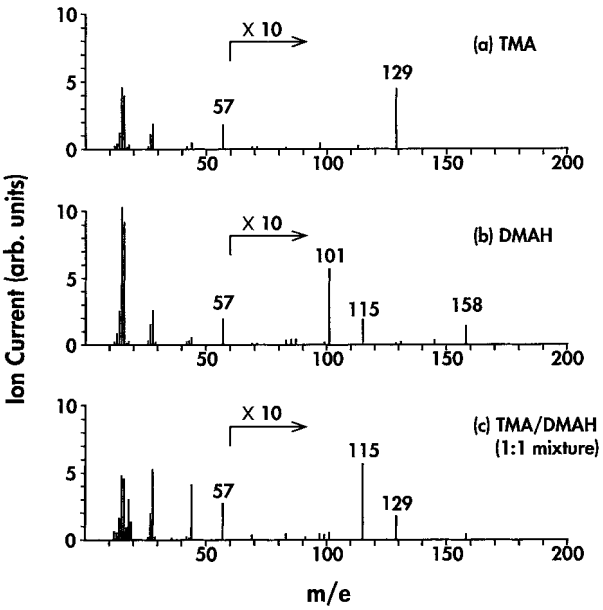

Figure 3 Quadrupole mass spectra for vapor of: (a) TMA; (b) DMAH; (c) a DMAH (50 mol%)/TMA (50 mol%) mixture. Ion current values were multiplied by 10 above a 60 mass number.

In the mass number range above 60, a major fragment of TMA appears at $m/z = 129$, and fragments of DMAH appear at mass numbers 101, 115 and 158, as shown in Fig 3(a) and (b). These fragments are almost the same as those reported in Refs 17 and 18. Since the parent ion mass number of the TMA dimer is 144 and that of the DMAH dimer is 116, each parent ion does not appear in the mass spectrum. During the ionization in the quadrupole mass filter, the TMA and DMAH dimers each tends to liberate a methyl group (mass number 15). The DMAH dimer also liberates a bridging hydrogen atom.[18] Hence, the dimeric TMA ($m/z = 144$) provides the main peak at 129, due to loss of a methyl group. Similarly, the dimeric DMAH (116) yields main peaks at 101 and 115 due to methyl group and hydrogen loss. DMAH also shows a mass number of 158, which comes from trimeric DMAH with a mass number of 174, by liberating a methyl group and a hydrogen atom. The vapor from the mixture shows major peaks at $m/z = 115$, 129 and 158, as indicated in Fig. 3(c). This pattern differs from the TMA and DMAH pattern superimposition, because the superimposition spectrum would have a higher 101 peak than the 115 peak. This difference strongly suggests that the mixture vapor contains the new molecular compound, based on the following considerations. First, the DMAH dimer should contribute only slightly to the peak at 115, because the peak at 101 from DMAH is very low, as indicated in Fig. 3(c). Secondly, even if the total contribution to the peak at 129 in the mixture comes from TMA dimer, the TMA dimer does not contribute to the peak at 115. Therefore, most of the peak strength at 115 must come from a new compound, other than the DMAH dimer or the TMA dimer. The mass number of 158 comes from trimeric DMAH in the mixture.

Quadrupole mass analysis can determine the mass of the new compound, as follows. We utilized a common property of TMA and DMAH, which appears in both fragmentation patterns: H and CH_3 loss. In the case of the mixture, the 115 and 129 fragments appeared as main peaks. Therefore, assuming that the new compound has the same fragmentation property, it should have mass numbers 116, 130 or 144, by summing 1 or 15 with the 115 or 129 fragments. Of these, the mass number 116 can be excluded, because the 101 fragment appears in a very small amount in the mixture vapor. The mass number 144 can also be excluded, because it does not cause the observed 115 fragment. Therefore, the new compound has been deduced to have the mass number 130, which can contribute to both 115 and 129 fragments. For the 129 fragments of the vapor in the mixture, the contribution from the TMA dimer and the new compound cannot be elucidated by this quadrupole mass analysis alone.

The chemical formula for the new compound has been deduced as follows. The structures for the TMA and DMAH dimers have been reported (Fig. 4).[19,20] At room temperature (about 300 K), thermal energy is not sufficiently high to cause drastic chemical structural changes in the TMA and DMAH mixture. For example, at 333 K, TMA gas consists of more than 97% dimers; even at 588 K, TMA gas consists of 96% monomers, which indicates that below 500 K the TMA decomposition rate is very low.[19] Therefore, only small structural changes in TMA dimers and DMAH dimers, to form other types of aggregates, should be considered. Generally, $(TMA)_x$ $(DMAH)_y$-type aggregation may occur in the mixture. According to the deduced mass number of 130, TMA–DMAH, $(CH_3)_3Al$–$(CH_3)_2AlH$, is the most probable chemical formula for the new compound. Hereafter, this compound is referred to as TDMA (trimethylaluminum dimethylaluminum hydride molecular aggregate). One of the TDMA conformers is shown in Fig. 4(c).

Although the stability of TDMA was not

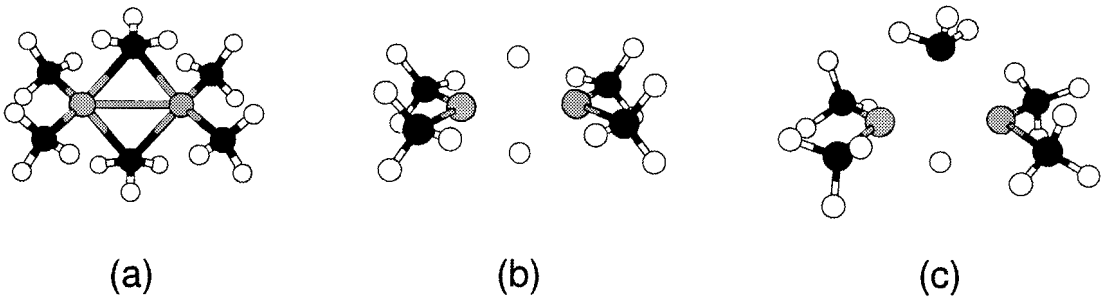

Figure 4 Schematic diagrams showing the molecular structures of (a) TMA dimer, (b) DMAH dimer and (c) TDMA.

investigated precisely, QMS samples of the same batch of liquid mixture at different times showed almost the same fragmentation patterns. Therefore, TDMA is considered to be stable for several weeks at least.

Ab-initio calculations

To investigate more precisely the molecular structure of the new compound, *ab-initio* orbital calculations were carried out. It is known that TMA exists as a dimer with two methyl groups forming bridges between the aluminum atoms.[19] It is also known that DMAH exists as a dimer with two hydrogen atoms forming bridges between the aluminum atoms.[20] It is, therefore, interesting to see what will happen when these alkylaluminum compounds with two different bridging atoms are mixed. *Ab-initio* calculations for TMA and DMAH dimers performed by Hiraoka *et al.*[21] proved that the dimers are more energetically stable than the two monomers. We have calculated the total energies of individual molecules of TDMA, TMA and DMAH (Table 1); conformers of dimeric DMAH have been evaluated by their total energies.

We have evaluated the total energies for five conformers of dimeric DMAH: (**1**) dihydrogen-bridged; (**2**) monohydrogen- and monomethyl-bridged; (**3**) dimethyl-bridged and dihydrogen-terminated on one Al; and (**4, 5**) dimethyl-bridged and monohydrogen-terminated on both Al (*trans*- and *cis*-) (Table 2). The results show that the dihydrogen-bridged DMAH dimer is the most

Table 1 Total energies and zero-point vibrational energies (hartree)

	Total energy		Zero-point energy
	HF/6–31 G**//HF/6–31 G**	MP2/6–31 G**//HF/6–31 G**	HF/6–31 G**
TMA	−360.7709367	−361.2778035	0.112034
DMAH	−321.7208202	−322.082333	0.081453
$(TMA)_2$	−721.5488354	−722.5866061	0.228609
$(DMAH)_2$	−643.4832318	−644.220014	0.168776

Table 2 Energy difference for $DMAH_2$ conformers (HF/6–31 G**//HF/6–31 G**)

Structure[a]	Total energy	Zero-point energy	ΔE (a.u)	ΔE (kcal mol^{-1})
1	−643.483232	0.168776	—	—
2	−643.467248	0.168144	0.015352	9.6
3	−643.449968	0.167794	0.032282	20.3
4	−643.449899	0.167922	0.032479	20.4
5	−643.450196	0.167933	0.032193	20.2

[a] **1**, dihydrogen-bridged; **2**, monohydrogen- and monomethyl-bridged; **3**, dimethyl-bridged and dihydrogen-terminated on one Al; **4, 5**, dimethyl-bridged and monohydrogen-terminated on both Al (**4**, *trans*; **5**, *cis*).

Table 3 Energy difference for TDMA conformers (HF/6–31 G** //HF/6–31 G**)

Structure[a]	Total energy	Zero-point energy	ΔE (a.u)	ΔE (kcal mol^{-1})
1	−682.517003	0.198581	0.017164	10.8
2	−682.499544	0.198286		

1, H,CH_3-bridged; **2**, CH_3,CH_3-bridged.

Table 4 Energetics

	ΔE (hartree)		ΔE_0 (kcal mol^{-1})
	HF/6–31 G** //HF/6–31 G**	MP2/6–31 G** //HF/6–31 G**	HF/6–31 G**
2 TMA → $(TMA)_2$	−0.006962	−0.030999	−16.6
2 DMAH → $(DMAH)_2$	−0.041591	−0.055345	−31.0
TMA + DMAH → TDMA	−0.025247	−0.043943	−24.4

stable; this coincides the experimental structure.[20] There are two conformers of TDMA, of which one is dimethyl-bridged (structure **1**) and the other hydrogen–methyl-bridged (structure **2**). We found that the latter is energetically favorable (Table 3). Dimerization or aggregation energies of TMA, DMAH and TDMA are listed in Table 4. The DMAH dimer has the largest dimerization energy, 31.1 kcal mol^{-1} (130 kJ mol^{-1}), the next is TDMA with 24.4 kcal mol^{-1} (102 kJ mol^{-1}), and the smallest is the TMA dimer, 16.5 kcal mol^{-1} (69 kJ mol^{-1}). Therefore dimerization of DMAH is considered to be more stable than that of the other species mentioned above. From these energy values, the energy difference (ΔE_0) is evaluated for the following equilibrium:

$$\frac{1}{2}(TMA)_2 + \frac{1}{2}(DMAH)_2 = TDMA - 0.6(\text{kcal mol}^{-1}) \quad [1]$$

Therefore, in the TMA/DMAH mixture it is considered that there is equilibrium between the TMA dimer plus the DMAH dimer and TDMA. Additionally, because Eqn [1] is exothermic, the equilibrium should be biased to the right-hand side.

FTIR analysis

Figure 5 shows infrared absorption spectra for (a) TMA, (b) DMAH, and (c) a TMA/DMAH mixture (3:7 in liquid mixture). The spectrum in Fig. 5(a) is essentially the same as that for TMA dimers in the gas phase in Ref. 22, but the FTIR spectra of DMAH and the mixture were measured for the first time in this experiment.

In order to assign these IR spectra, the harmonic frequencies were calculated at HF/6–31G**. The assignments are listed in Table 5 for TMA, Table 6 for DMAH and Table 7 for TDMA. Frequencies calculated at HF are known to show large values. The scaling factor recommended is 0.8929 for HF/6–31G*.[23] We employed this value for HF/6–31G** because it best resembles the basis sets. The vibrational mode assignment in the present study was determined by using a visualization of the normal mode. There are some discrepancies between our assignment and Kvisle's in Ref. 22. TMA's IR spectrum shows the characteristic CH_3^b(*b* means bridge, hereafter) deformation at 567.1 cm^{-1} and CH_3^brocking modes at 775.4 cm^{-1}, which provide evidence of methyl crosslinks between two Al atoms in the TMA dimer.

When the FTIR spectrum for DMAH (Fig. 5b) was compared with that for TMA (Fig. 5a), CH_3 asymmetric stretching modes (at around 2950 cm^{-1}) and CH_3^t(*t* means terminal, hereafter) deformation (707.9 cm^{-1}) were commonly observed in both spectra. On the other hand, the Al–C^b-stretching and CH_3^bdeformation modes observed in the TMA dimer were not observed in the DMAH spectrum. Therefore, the DMAH dimer had no bridging methyl, and had crosslinks through hydrogen atoms, which agrees with the results obtained by gas-phase electron-beam diffraction,[20] and also with those of our total energy calculations as described above.

Characteristic vibration spectra for DMAH have

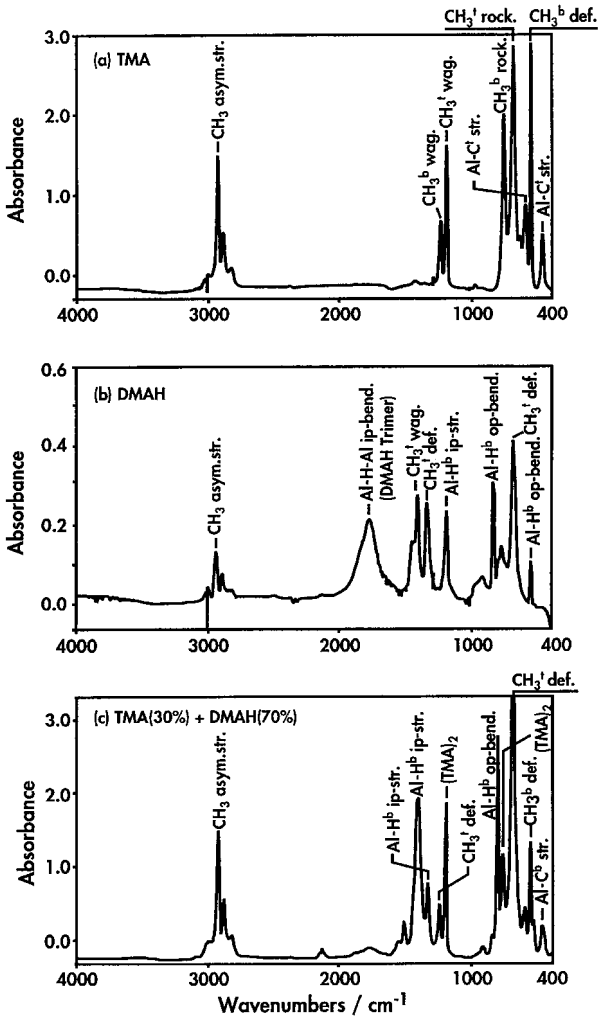

Figure 5 Infrared absorption spectra at room temperature for vapor of: (a) TMA; (b) DMAH; (c) a DMAH (70 mol%)/TMA (30 mol%) mixture.

also been found at 1790, 1424, 1352, 1206, 934, 852, 791, 708 and 570 cm^{-1}. Al–H–Al bending modes, 852 and 570 cm^{-1} (out-of-plane) and CH_3^tdeformation (1425, 1352, 708 cm^{-1}) agree within 5 cm^{-1} error. Although the frequencies differ by 60, 150, and 210 cm^{-1}, the 791, 1206 and 934 cm^{-1} peaks may be assigned to the Al–H–Al bending mode (the first out-of-plane, the latter two in-plane). A broad peak at 1790 cm^{-1} could not be assigned to the DMAH dimer, because there is no predicted frequency around here. We have also estimated vibrational frequencies for DMAH trimers by *ab-initio* calculations, which show there is a strong Al–H–Al degenerate bending peak at 1754 cm^{-1}. Therefore we attributed the 1790 cm^{-1} peak to the Al–H–Al degenerate bending peak of the DMAH trimer.

The spectra for the TMA and DMAH mixture are expected to be a superimposition of the spectra for the TMA dimer, the DMAH dimer and TDMA, weighted by each molar fraction. In order to extract the TDMA spectrum, the spectra for pure TMA and pure DMAH have been subtracted from that for the mixture, as much as possible, under the restriction that the resultant spectrum should not yield negative optical density in the wavenumber range between 400 and 4000 cm^{-1}. The TMA component in the mixture spectrum was estimated at 0.52 with the pure TMA spectrum as the unit. Similarly, the DMAH component in the mixture spectrum was estimated at 0.83, with the pure DMAH spectrum as the unit.

The difference spectrum in Fig. 6 shows characteristic peaks at 1414, 1339, 1207, 820 and 703 cm^{-1}. The assignments are listed in Table 7. The scaling factor for HF/6–31G* is employed in the same manner as when the DMAH dimer was assigned. The three peaks, 1414, 1339 and 820 cm^{-1}, can be assigned to Al–H–Al bending modes; the former two in-plane the last an out-of-plane mode. A very strong peak at 703 cm^{-1} is assigned to CH_3^tdeformation. The 1207 cm^{-1} peak cannot be assigned to any TDMA vibrational modes, so we believe there are residual TMA components.

Evaluation of the TDMA fraction in the mixture

We assume that TDMA is a single residual ingredient in the difference spectrum in Fig. 6. Then how many TDMA molecules are there in the TMA and DMAH mixture? Following the Beer–Lambert law, the TDMA molar concentration C is represented by Eqn [2],

$$\alpha = \epsilon CL \qquad [2]$$

where α, ε and L represent the optical density, molar absorption coefficient and absorption-cell length. The TDMA C–H asymmetric stretching mode optical density was obtained from the difference spectrum in Fig. 6. Table 8 lists the measured optical density, the evaluated molar fraction and the molar absorption coefficient for each vapor. The ε value for the C–H stretching in TDMA was considered to be the average of the TMA and DMAH values, if it is assumed that the molar absorption coefficient for C–H stretching is proportional to the number of methyl groups. Especially since a TMA dimer has six methyl

Table 5 Vibrational frequencies for $(TMA)_2$

Obs.	Int.	Wavenumber (calc.)* sf†	Calc.int.	Our assignment	Their assignment*
478.3	m‡	518.91	119.8	Al–C^t*str.*	Al–C^b*str.*
567.1	s	579.99	203.0	CH_3^b*def.*	Al–C^t*str.*
600.5	m	608.53	38.7	Al–C^t*str.*	CH_3^t*rock*
650.0	vw	622.52	53.5	$CH_3^{b,t}$*def.*	CH_3^t*rock*
702.1	vs	702.27	202.7	CH_3^t*rock.*	Al–C^t*str.*
		702.51	238.4	CH_3^t*rock*	
775.4	s	762.29	212.3	CH_3^b*rock*	CH_3^b*rock*
1207.4	s	1234.66	33.0	CH_3^t*wag.*	CH_3^t*sym.def.*
		1235.64	87.7	CH_3^t*wag.*	
1253.7	m	1257.33	67.7	CH_3^b*wag.*	CH_3^b*sym.def.*
2839.2	w	2856.96	28.4	CH_3^b*asym.str.*	2xCH_3 *asym. def.*
2900.9	m	2867.21	125.2	CH_3^t*asym.str.*	CH_3 *sym.str.*
2941.4	s	2871.82	120.5	CH_3^t*asym.str.*	CH_3 *asym.st.r*

*Ref. 22.
†Scaling factor of Ref. 23.
‡Abbreviations: vw, very weak; w, weak; m, medium; s, strong; vs, very strong; t, terminal; b, bridge; str, stretching; rock, rocking; sym, symmetrical; def, deformation; asym, antisymmetrical.

groups, and a DMAH dimer has four methyl groups, TDMA is considered to have five methyl groups, from the discussion of the TDMA structure in sections on QMS and FTIR analysis. Individual ε values for TMA and DMAH were obtained, based on the observed optical density for the C–H stretching band and the concentration calculated from its vapor pressure (TMA: 11.6 Torr;[9] DMAH: 1.9 Torr[8]), assuming the ideal gas laws. Molar concentration C for TDMA can be estimated using Eqn [2]. The TDMA molar fraction in the DMAH (70 mol% as a monomer) + TMA (30 mol% as a monomer) vapor mixture was estimated to be at least 50 mol%. If there are 30 mol of TMA and 70 mol of DMAH and all the TMA were consumed to produce TDMA, and 30 mol of DMAH were consumed to leave 40 mol of DMAH, then 20 mol of $(DMAH)_2$ would be produced. So the molar ratio of TDMA to $(DMAH)_2$ should become 60:40. Although not all the TMA is consumed in this case, it is consistent that the equilibrium in Eqn [1] proceeds to the right side.

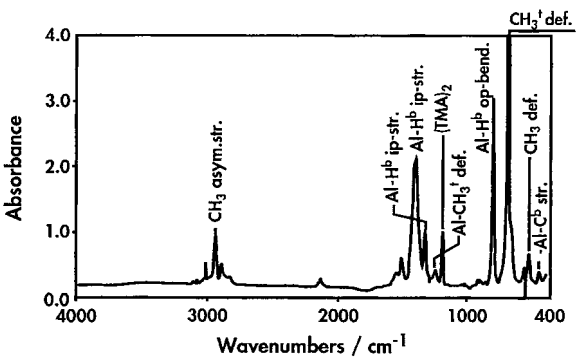

Figure 6 TDMA infrared absorption spectrum, obtained by subtracting pure TMA and pure DMAH spectra from the spectrum of a DMAH (70 mol%) and TMA (30 mol%) mixture.

The reaction probability of the TDMA is considered to be of the same order as that of the DMAH, because the CVD precursor of the vapor from the liquid mixture of TMA and DMAH (3:7 fraction) contains 11% of DMAH at most, and the CVD rate was of the same order as that from the pure DMAH. In addition, since TMA is known to cause no CVD reaction at a substrate temperature of 240 °C, the TDMA in the vapor from the mixture must contribute to the Al deposition.

So far, we have discussed the existence of TDMA in gas phase. A liquid mixture of TMA and DMAH has preliminarily been analyzed by an NMR (nuclear magnetic resonance) method, and some hydrogen peaks which confirm the existence of TDMA have been observed in the mixture.

Table 6 Vibrational frequencies for $(DMAH)_2$

Obs.	Int.	Wavenumber (calc)* sf	Calc.int.	Assignment
570.0	m	563.17	3.99	Al–H^b*op.bend*
707.9	vs	705.72	318.2	CH_3^t*def*.
790.8	w	731.70	0.0002	Al–H^b*ob.twist*
851.6	s	849.69	473.5	Al–H^b*op.bend*
933.5	w	1147.13	482.2	Al–H^b*ip.bend*
1205.5	s	1353.27	1695.7	Al–H^b*ip.str.*
1352.1	s	1411.75	4.8	CH_3^t*def*.
1423.5	s	1417.79	2.8	CH_3^t*wag*.
1788.0	bs			Al–H$(DMAH)_3$
2904.8	w	2818.08	32.9	CH_3^t*sym.str*.
		2818.51	24.4	CH_3^t*sym.str*.
2951.1	m	2876.17	108.5	CH_3^t*asym.str*.
2960.7	s	2887.80	84.0	CH_3^t*asym.str*.
		2889.98	25.3	CH_3^t*asym.str*.

Abbreviations; bs, broad strong; op, out-of-plane; ip, in-plane; bend, bending; twist, twisting; wag, wagging: see also Table 5.

Table 7 Vibrational frequencies for TDMA

Obs.	Int.	Wavenumber (calc)* sf	Calc.int.	Assignment
461.4	m	427.21	43.2	Al–C^b*str.* or $(TMA)_2$
540.1	m	500.86	96.8	CH_3*def.* or $(TMA)_2$
703.1	vs	696.33	149.2	CH_3^t*def*.*or*$(TMA)_2$
819.7	s	808.64	313.3	Al–H^b*op.bend*
1207.4	m			$(TMA)_2$
1253.7	w	1233.38	59.7	$AlCH_3^t$*def*.*or*$(TMA)_2$
1338.6	m	1293.99	297.2	Al–H^b*ip.str.*
1413.8	s	1378.04	788.6	Al–H^b*ip.str.*
1518.0	m	1417.19	47.8	Al–H^b*ip.str.* + CH_3*def.*
2839.2	w	2813.91	24.9	CH_3^t*sym.str*.
2900.9	m	2871.74	87.4	CH_3^t*asym.str*.
2945.3	s	2879.11	35.3	CH_3^t*asym.str*.
		2881.78	55.7	CH_3^t*asym.str*.

Abbreviations; see Tables 5 and 6.

Table 8 Characteristic values for TDMA, TMA and DMAH in the mixture of TMA and DMAH (3:7 in liquid mixture).

	α	ε (l mol^{-1} cm^{-1})	C (mmol l^{-1})	Molar fraction
TDMA	0.78	190	0.410	0.50
$(TMA)_2$	0.85	265	0.321	0.39
$(DMAH)_2$	0.10	116	0.086	0.11

SUMMARY

A new type of precursor, whose viscosity is substantially lower than that of DMAH, has been developed for Al-CVD by blending dimethylaluminum hydride (DMAH) and trimethylaluminum (TMA). The precursor vapor has been found to contain a new molecular compound between a

DMAH monomer and a TMA monomer (TDMA). QMS analysis revealed the structure of TDMA. From FTIR analysis the molar fraction of TDMA in the mixture of DMAH and TMA was estimated. The total energy and vibrational frequency of TDMA, the TMA dimer and the DMAH dimer were evaluated from *ab-initio* molecular orbital calculations. Good applicability to Al-CVD of the precursor has been revealed.

Acknowledgements The authors thank Kazuo Tateishi of NEC Environment Engineering for FTIR analysis, Professor Mitsuo Tasumi of Saitama University for his valuable advice in regard to FTIR data-processing and Sigehiko Tsukamoto of the Hokkaido Industrial Research Institute for his useful discussion on *ab-initio* calculations.

REFERENCES

1. N. Suzuki, C. Anayama, K. Masu, K. Tsubouchi and N. Mikoshiba, *J. Appl. Phys.* **25**, 1236 (1986).
2. M. L. Green, R. A. Levy, R. G. Nuzzo and E. Coleman, *Thin Solid Films* **114**, 367 (1984).
3. R. A. Levy, M. L. Green and P. K. Gallagher, *J. Electrochem. Soc.* **131**, 2175 (1984).
4. T. Amazawa and H. Nakamura, *Extended Abstract of the 18th Conference on Solid State Devices and Materials, Tokyo, 1986*, pp. 755–756.
5. T. Amazawa, H. Nakamura and Y. Arita, IEEE IEDM Tech. Digest, 1988, p. 442.
6. T. Shinzawa, K. Sugai, S. Kishida and H. Okabayashi, *Mater. Res. Soc. Symp. Proc. VLSI V*, 1990, p. 377.
7. K. Tsubouchi, K. Masu, N. Shigeeda, T. Matano, Y. Hiura and N. Mikoshiba, *Appl. Phys. Lett.* **57**(12), 1221 (1990).
8. T. Wartik and H. I. Schlesinger, *J. Am. Chem. Soc.* **75**, 835 (1953).
9. G. B. Stringfellow, *Organometallic Vapor Phase Epitaxy: Theory and Practice*, Academic Press, New York, 1989, p. 27.
10. Y. Ohshita, F. Uesugi and I. Nishiyama, *J. Crystal Growth* **115**, 551 (1991).
11. Y. Teraoka, H. Aoki, E. Ikawa, T. Kikkawa and I. Nishiyama, *J. Vac. Sci. Technol.* **B13**, 2197 (1995).
12. P. Pulay, in: *Modern Theoretical Chemistry*, Vol. **4**, Schaefer, H. F. III (ed.), Plenum, New York, 1977, Chapter 4.
13. J. A. Pople and R. Krishnan, *Int. J. Quantum Chem.* **14**, 91 (1978).
14. R. Krishnan, M. J. Frish and J. A. Pople, *J. Chem. Phys.* **72**, 4244 (1980).
15. W. J. Hehre, L. Radom, P. von, R. Schleyer and J. A. Pople, in: *Ab Initio Molecular Orbital Theory*, Wiley, New York, 1986.
16. M. J. Frisch, G. W. Trucks, H. B. Schlegel, P. M. W. Gill, B. G. Johnson et al., Gaussian 94, Gaussian Inc., Pittsburgh, PA, 1995.
17. J. Tanaka and S. R. Smith, *Inorg. Chem.* **8**, 265 (1969).
18. D. B. Chambers, G. E. Coates, F. Glockling and M. Weston, *J. Chem. Soc. (A)* 1712 (1969).
19. A. Almenningen, S. Halvorsen and A. Haarland, *Acta Chem. Scand.* **25**, 1937 (1971).
20. G. A. Anderson, A. Almenningen, F. R. Forgaard and A. Haaland, *Chem. Commun.* 480 (1971).
21. Y. S. Hiraoka and M. Mashita, *J. Cryst. Growth* **145**, 473 (1994).
22. S. Kvisle and E. Rytter, *Spectrochim. Acta* **40A**, 939 (1984).
23. J. A. Pople, A. P. Scott, M. W. Wong and L. Radom, *Isr. J. Chem.* **33**, 345 (1993).

